

Evaluation of bone repair of defects treated with Bio-Oss® and platelet rich fibrin (PRF)

Avaliação da reparação óssea de defeitos tratados com Bio-Oss® e PRF

Eduardo Antonio Chelin SUAREZ¹ , Letícia Cavassini TORQUATO¹ , Ludmilla Oliveira MANTOVANI¹ , Kauê Alberto PEREIRA^{1,2} , Clarissa Carvalho Martins MACIEL¹ , Nataly Domingues ALMEIDA¹ , Camilla Magnoni Moretto NUNES¹ , Maria Aparecida Neves JARDINI¹ , Mauro Pedrine SANTAMARIA¹ , Andrea Carvalho DE MARCO¹ 

1 - Universidade Estadual Paulista, Departamento de Diagnóstico e Cirurgia. São José dos Campos, SP, Brazil.

2 - Fundação Universitária Vida Cristã, Disciplina de Periodontia. Pindamonhangaba, SP, Brazil.

How to cite: Suarez EAC, Torquato LC, Mantovani LO, Pereira KA, Maciel CCM, Almeida ND, et al. Evaluation of bone repair of defects treated with Bio-Oss® and PRF. *Braz Dent Sci*. 2025;28(3):e4802. <https://doi.org/10.4322/bds.2025.e4802>

ABSTRACT

Objective: The aim of this study was to evaluate the bone repair of critical size defects in rats treated with bovine bone matrix (Bio-Oss®) and platelet, and leukocyte-rich fibrin (L-PRF) through histomorphometric and Immunohistochemical analysis. **Material and Methods:** Thirty adult rats (Albinus, Wistar), 90 days old, were used. Two critical bone defects of 5mm in diameter were made in the calvaria. The animals were divided into 4 (four) groups: those with C-Blood clot, B-Bio-Oss®, PRF-PRF, B+PRF-Bio-Oss®+PRF. Each group was subdivided into observation periods of 30 and 60 days. All data were statistically analyzed, with a significance level of 5%. **Results:** All groups presented similar results regards the proportion of bone neoformation. At 30 days, in the proportion of lamellar neoformation, PRF showed a statistical difference with B (Bvs.PRF, $p=0.0256$). Regarding the closure of the defect, at the 30 days mark the PRF showed a difference from C (PRFvs.C, $p=0.0374$), and at the 60 days, the B showed difference to GC (Bvs.C, $p=0.0374$). summarize the article's main findings. **Conclusion:** Through descriptive statistics, it was possible to observe that PRF has a positive action on the initial bone neoformation process. The association Bio-Oss® and PRF seems to be related to the maintenance of the bone neoformation architecture. However, more studies are needed to confirm this finding.

KEYWORDS

Biocompatible materials; Bone regeneration; Osteogenesis; Platelet rich fibrin; Tissue engineering.

RESUMO

Objetivo: O objetivo deste estudo foi avaliar a reparação óssea de defeitos críticos em ratos tratados com matriz óssea bovina (Bio-Oss®) e fibrina rica em plaquetas e leucócitos (PRF) por meio de análises histomorfométrica e imuno-histoquímica. **Material e Métodos:** Foram utilizados trinta ratos adultos (Albinus, Wistar) com 90 dias de idade. Foram realizados dois defeitos ósseos críticos de 5 mm de diâmetro na calvária. Os animais foram divididos em 4 (quatro) grupos: C-Coágulo sanguíneo, B-Bio-Oss®, F-PRF e B+F-Bio-Oss®+PRF. Cada grupo foi subdividido em períodos de observação de 30 e 60 dias. Todos os dados foram analisados estatisticamente, com um nível de significância de 5%. **Resultados:** Todos os grupos apresentaram resultados semelhantes em relação à proporção de neoformação óssea. Aos 30 dias, na proporção de neoformação lamelar, o grupo F apresentou diferença estatística em relação ao grupo B (B vs F, $p=0.0256$). Em relação ao fechamento do defeito, aos 30 dias, o grupo F apresentou diferença em relação ao grupo C (F vs C, $p=0.0374$) e, aos 60 dias, o grupo B apresentou diferença em relação ao grupo C (B vs C, $p=0.0374$). **Conclusão:** Através da estatística descritiva, foi possível observar que o PRF tem uma ação positiva no processo inicial de neoformação óssea. A associação entre Bio-Oss® e PRF parece estar relacionada à manutenção da arquitetura da neoformação óssea. No entanto, mais estudos são necessários para confirmar esse achado.

PALAVRAS-CHAVE

Materiais biocompatíveis; Regeneração óssea; Osteogênese; Fibrina rica em plaquetas; Engenharia tecidual.

INTRODUCTION

Autogenous bone is recognized as the gold standard for bone grafting, providing osteogenic cells, extracellular matrix, and molecular signals for bone induction and differentiation [1,2]. However, the removal of autogenous grafts implies a second donor surgical site and increases patient morbidity [3,4].

Ideally, bone substitute materials should present good bone integration, osteoinduction, and long-term stability [5]. One of the grafts that have been showing good results, together with good clinical documentation, is the Bio-Oss® xenograft (Geistlich Biomaterials GmbH), which consists of a bone mineral matrix of natural origin, porous and bovine, cortical, or spongy [6,7]. Its use offers excellent compatibility with the human bone matrix and stimulates osteogenesis. However, xenograft bone particles are not resorbable [8,9].

Platelet Rich Fibrin (PRF), described by Choukroun in 2001, is a platelet concentrate, classified as the second generation, responsible for the following chain of events: increased collagen production, cell mitosis, angiogenesis, cell recruitment, induction of cell differentiation, among others. The use of PRF has shown interesting clinical properties, such as promoting a better and faster repair of surgical wounds and showing its application in oral and maxillofacial surgery [10,11].

Some studies describe the benefits of PRF when used as a sole graft material or combined with other bone substitutes, such as lyophilized bone, deproteinized bovine bone, and autogenous bone, demonstrating optimistic results [12-16]. The association of the osteoconductive and osteogenesis function of bovine xenografts with PRF cytokines and growth factors shows promise in the attempt of bone growth [9,17].

Although positive effects of the bovine bone matrix with PRF have been demonstrated on bone cell proliferation, the evidence for the therapeutic efficacy of this combination is still controversial [18]. Thus, this study aimed to evaluate, through histomorphometric and Immunohistochemical analysis, the bone repair of critical defects in rats treated with bovine bone mineralized bone matrix and platelet-rich fibrin.

MATERIAL AND METHODS

Animals and experimental groups

This study was carried out per the Ethical Principles for Animal Experimentation, adopted by the National Council for Animal Experimentation – CONCEA, and approved by the Research Ethics Committee of the São José dos Campos Institute of Science and Technology/UNESP (nº 07/2019). The description of this work was done following the Animal Research guidelines: Reporting in vivo experiments – ARRIVE guidelines 2.0 [19].

Thirty adult male rats (*Rattus norvegicus*, Albinus variation, Wistar), 90 days old, weighing approximately 300g, supplied by the Central Animal Facility of Unesp – Campus de Botucatu-SP, were used. Rats were stored in appropriate cages and received diet and water *ad libitum*. Of the 30 animals, 06 were destined as blood donors for the preparation of Platelet Rich Fibrin (PRF); the other 24 rats were randomly divided by a draw into four (4) groups: C – bone defect + blood clot, B – bone defect + Bio-Oss®, PRF – bone defect + PRF and B+PRF – bone defect + Bio-Oss® + PRF. Each group was subdivided according to observation periods of 30 and 60 days (Figure 1).

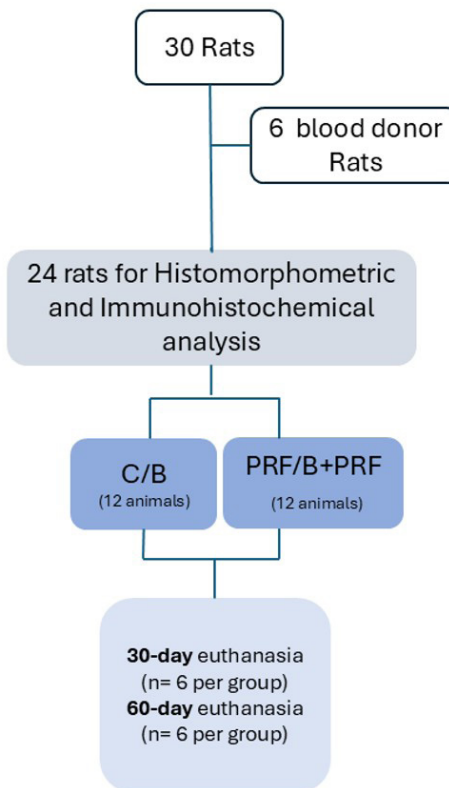


Figure 1 - Study Design Flowchart.

Anesthetic procedure

For surgery and euthanasia, the animals were anesthetized with a solution of 10mg/kg of 2-(2,6-xylidine)-5-6-dihydro-4H-1,3 thiazine hydrochloride (Anasedan – Bayer do Brasil) and 100mg/kg of ketamine base (Dopalen – Agribands do Brasil), intramuscularly. As analgesic, a solution of 6mg/kg of Tramal (tramadol hydrochloride – Medley) was administered orally before surgery and followed every 24 hours for 5 days.

Surgical procedure

A longitudinal incision was made in the skin, about 1 cm long, along the sagittal suture, exposing the calvaria.

On each side of the calvaria, two critical size bone defects, with 5 mm in diameter, were performed [20,21], using an electric motor that allows controlled speed at 800 RPM and one trephine drill under constant irrigation with sterile saline. Then, using a blade-shaped ultrasound tip (W1-0-CVDentus) in a piezo surgical device (DentSurg CVDentus São José, SP, Brazil) under constant irrigation, an “L”-shaped marking was made 2 mm from the edge of each defect in the place corresponding to its largest diameter, the marking was then filled with amalgam. After this step, the designated treatment was applied.

The subcutaneous tissue and the skin were sutured with 4.0 silk thread, and an anti-inflammatory analgesic medication was administered (Meloxicam 0.2% at a dose of

2mg/kg, subcutaneously every 24h for three (3) days) and the Pentabiotic (0.01ml each 100g intramuscularly in a single dose). The day of surgery counted as day zero.

Treatments

Bio-Oss® (Geistlich Biomaterials GmbH) is a xenogeneic bone substitute, the granulation used in this study was 0.25-1.0 μ m in diameter – 0.5g [6,7].

To obtain platelet-rich fibrin, the six (6) animals initially foreseen were used as donors. Blood collection was performed by intracardiac puncture with the animal properly anesthetized. The volume of blood extracted from each donor animal was 10 ml. Blood from each animal was processed to obtain PRF membranes according to the Choukroun protocol [9]. Blood was collected in plastic tubes with silica (9ml) and immediately placed in a centrifuge (Kasvi-Brasil), where they centrifuged for 12 minutes at a speed of 2500 rpm [18,22].

After centrifugation, the tubes were removed from the centrifuge and placed in the support, from which the fibrin clots, located in the central region of each tube, were carefully removed (Figure 2). The PRF membrane, considered to be rich in growth factors, was used to fill the bone defects or as a membrane covering Bio-Oss® (Figure 3). After blood donation, the animals were euthanized.

B right bone defect (PRF) and left bone defect filled by Bio Oss and PRF(B+PRF).

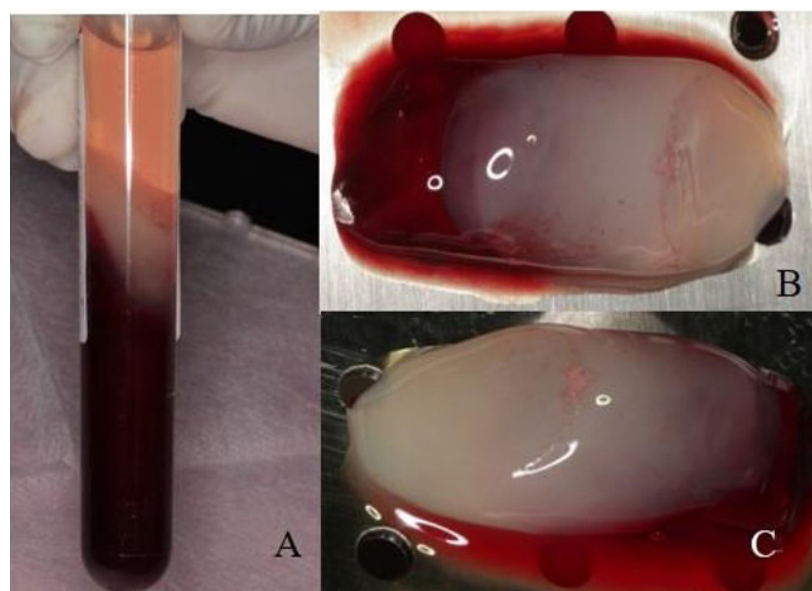


Figure 2 - A= three phases of platelet aggregate, B= Platelet-rich fibrin.

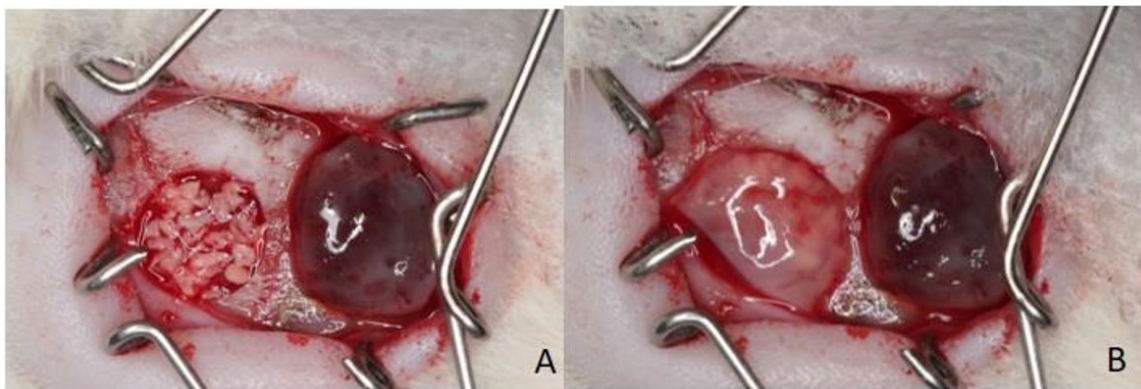


Figure 3 - A: Left bone defect filled with Bio-Oss before being covered with PRF membrane (B+PRF group). The right bone defect covered with PRF membrane (PRF group). B: In the subsequent step, the left bone defect previously filled with Bio-Oss covered with PRF membrane (B+PRF group), and the right defect covered with PRF membrane (PRF group).

Euthanasia

Animals were euthanized after their respective observation periods of thirty (30) and sixty (60) days; for this, a triple dose of anesthetic (mixture of ketamine and xylazine) was used, indicated for surgical procedures, followed by decapitation to remove the calvaria.

Twenty-four specimens that followed for histomorphometric and immunohistochemical analysis were fixed in 10% formalin ($n=6$), covering periods of thirty (30) and sixty (60) days.

Histological and histomorphometric analysis

For histological and histomorphometric analyses, the operated area was fixed in 10% formalin for the maximum period of 48 hours. Each specimen was cataloged. The decalcification process was made with 20% formic acid (Merck KGaA, in Darmstadt, Germany) for approximately seven days. After decalcification, specimens were embedded in paraffin.

Longitudinal cuts were performed on the $5\mu\text{m}$ thick pieces in a semi-serial way. In total, ten (10) slides were made from each specimen, then the sections were stained with hematoxylin-eosin and examined under light microscopy.

Three sections of each specimen were selected for image capture, the photos were taken using an Axiophot 2 light microscope (Carl Zeiss Oberkochen, Germany) coupled with an AxioCam MRC 5 digital camera (Carl Zeiss Oberkochen, Germany). A single examiner captured the images that received codes and were later analyzed by another examiner, allowing data to be blinded.

Histomorphometric analysis was performed by a single properly calibrated examiner.

Histomorphometric analysis was performed using the computer program Axio Vision Release 4.7.2. The criterion used to standardize the analysis of digital images was to delimit the total area of the defect (in mm^2) from the identification of the surgical edges on the right and left and the internal and external surfaces, the edges were identified by the difference between the neoformed bone and the original bone [23], this delimited area was considered as 100%. Therefore, the areas of bone neoformation within the defects were calculated as a percentage of the total area, and the areas corresponding to the particles of biomaterial remaining in the defect were not counted. Then, the following measurements were taken of the neoformation area (NA), the lamellar bone neoformation area (LBNA), the intramembranous bone neoformation area (IBNA), and the distance between neoformed bone edges (DBE-NB), these measurements were described previously [24].

Immunohistochemical analysis

Longitudinal cuts were performed on the $4\mu\text{m}$ thick pieces in a semi-serial way. Were prepared and mounted on slides pre-treated with 3-aminopropyltriethoxysilane (Sigma Chemical CO., St. Louis, USA). The histological sections were deparaffinized in xylene and rehydrated through a descending ethanol series. Antigen retrieval was performed by immersing the slides in citrate buffer, pH 6.0 (EP-12-20557 Easy Path), within a pressurized chamber (Decloaking Chamber®, Biocare Medical, USA) using two temperature cycles: 93°C for 4 minutes and 70°C for 25 seconds. Subsequently, the slides were washed in 0.1 M PBS-Triton, pH 7.4, and immersed in 3% hydrogen peroxide for 30 minutes.

The slides were divided into three batches, each incubated with one of the following primary antibodies: anti-RANKL (1:100, Goat anti-RANKL, SC-7628, Santa Cruz Biotechnology, USA), anti-OPG (1:200, Goat anti-OPG, SC-8468, Santa Cruz Biotechnology, USA), and anti-TRAP (1:100, Goat anti-TRAP, SC-30833, Santa Cruz Biotechnology, USA). The primary antibodies were diluted in antibody diluent solution (Spring ADS-125), and the slides were placed in a humid chamber for 16–18 hours at 4°C. Histological sections were then incubated with Histofine secondary antibody (Easy Link one EP-12-20501) for 30 minutes at room temperature. Visualization was achieved using the chromogen 3,3'-tetrachloride diaminobenzidine (DAB Chromogen Kit®, USA), followed by counterstaining with Harris hematoxylin. As a negative control, slides underwent the same procedures without primary antibodies.

A semi-quantitative analysis of immunolabeling localized exclusively in the newly formed bone within the defect was performed. In this region, cells per area were counted, and the following scores were established: Scores ranged from 0 (no expression) to 4 (very intense expression) [25].

Statistical analysis

The histological and histomorphometric analysis data obtained for the proportional variables of bone neoformation (%) in NA,

LBNA and IBNA, and the distance between neoformed bone edges (mm) DBE-NB were submitted for exploratory analysis. The data followed a non-parametric distribution. Therefore, the Kruskal-Wallis test was used as inferential statistics, followed by the Dunn test for multiple comparisons, and the Wilcoxon signed-rank test, the value adopted for the confidence level was 5%.

The data from the immunohistochemical analysis was submitted to the Kruskal Wallis test, Two-way ANOVA and the Sidak test for multiple comparisons. A significance level of 5% was adopted. The tests were performed by MINITAB (Minitab, version 12.0, 1998) and GraphPad PRISM (version 6, 2013) programs.

RESULTS

All twenty-four (24) rats followed the experiment period with good health status and had their data collected.

Descriptive histological analysis

Within 30 days after surgery, it was possible to observe the presence of bone neoformation in all specimens, generally concentrated in the regions close to the edges of the surgical defect (Figure 4). In some specimens of group B-30 days, it was possible to visualize new bone formed between the spaces of the remaining particles of biomaterial

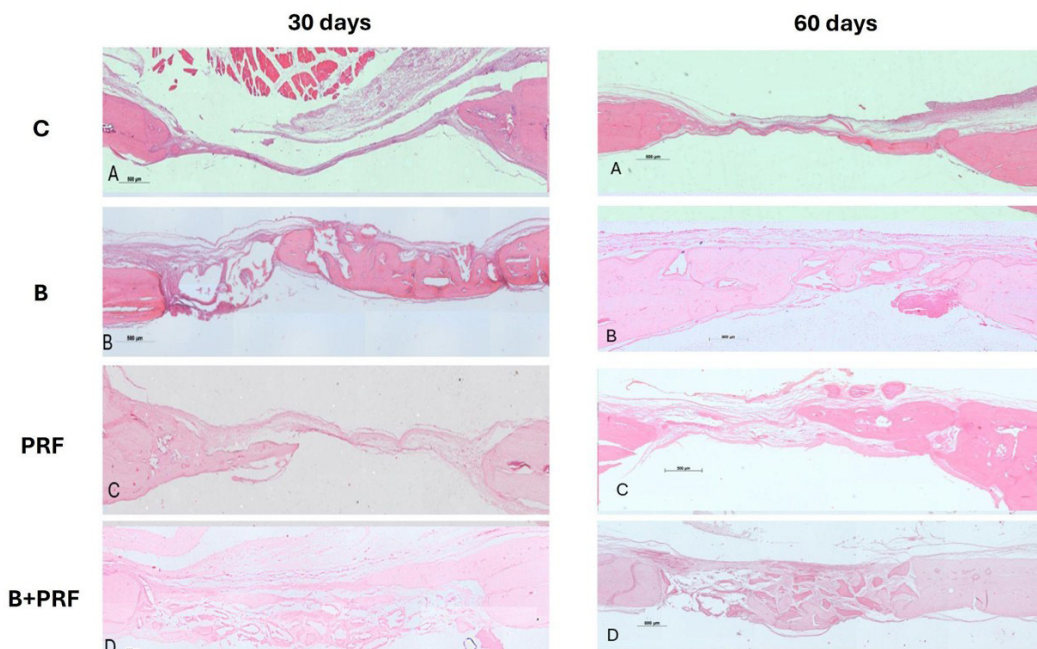


Figure 4 - Photomicrograph of the panoramic view of the surgical defect (hematoxylin and eosin staining, original magnification X5). (A) group C, (B) group B, (C) group PRF, (D) group B+PRF.

(Figure 4B), in the group B+PRF, it is possible to observe new bone formed in a disorganized way beside and above the edge of the surgical defect, with blood vessels (Figure 4D).

Within 60 days, most specimens had bone neoformation. In groups C and B, it was possible to notice a narrow band of newly formed bone along almost the entire length of the surgical defect, however thinner than the original bone of the calvaria. It was also possible to observe dense connective tissue and inflammatory infiltrate that extended throughout the surgical defect (Figures 4A* and 4B*). In specimens from group PRF – 60 days, it was possible to observe pronounced bone neoformation in some specimens but concentrated in the region of the defect border (Figure 4C*).

In specimens from Group B and Group B+PRF, it was possible to notice the presence of spaces that would be occupied by the biomaterial and/or residual particles of the biomaterial (Figures 4B*, and 4D*).

Histomorphometric analysis

At 30 and 60 days, no statistically significant intragroup differences were observed between the treatment modalities in terms of the neoformation area (NA). However, Group B at 60 days exhibited a significantly greater increase compared to Group B 30 days (B30 vs. B60; $p = 0.0313$) (Figure 5).

In the measure of the proportion of the lamellar bone neoformation area (LBNA), at 30 days, group PRF showed a statistically significant difference relative to group B (B vs. PRF, $p = 0.0256$), while the remaining groups were statistically similar. At 60 days, there was no statistically significant difference between the treatment modalities. Only group B showed a statistically significant difference within the intragroup comparison (B 30 vs. B 60, $p=0.0313$) with significant improvement within the variable (Figure 6).

In the measure of the intramembranous bone neoformation area (IBNA), at 30 and 60 days, the treatment groups presented similar statistical results, there was no statistically significant difference in the intragroup or intergroup comparisons (Figure 7).

Regarding the variables obtained within the distance between neoformed bone edges (DBE-NB), at 30 days, group C presented a statistically

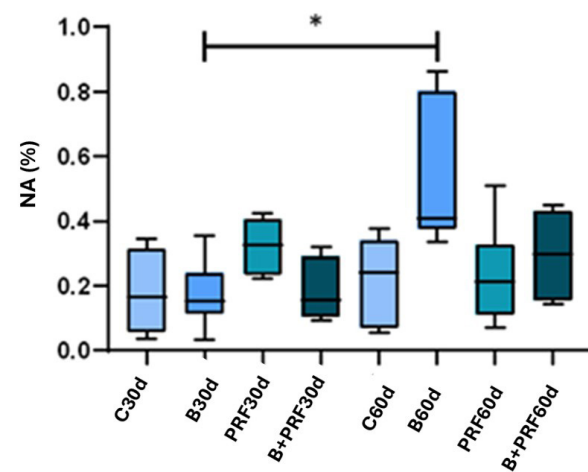


Figure 5 - Maximum and minimum values, median, 1st and 3rd quartiles of the Bone Neoformation Area (NA) in percentage. Statistically significant intragroup difference for Group B (*).

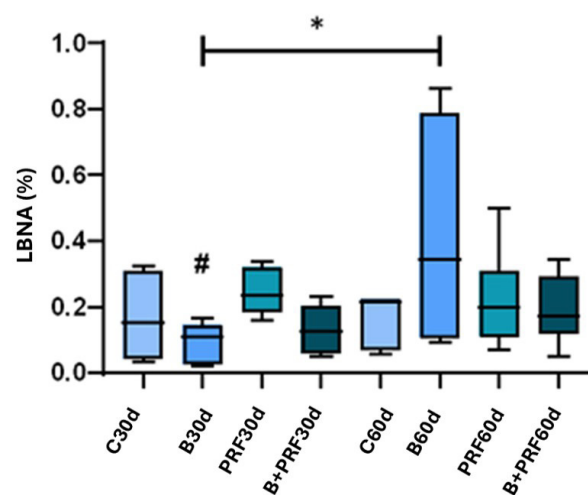


Figure 6 - Maximum and minimum values, median, 1st and 3rd quartiles of the Lamellar Neoformation Area (LBNA) in percentage. Statistically significant difference for Group B at 30 and 60 days. Statistically significant difference between PRF and B Groups at 30 days.

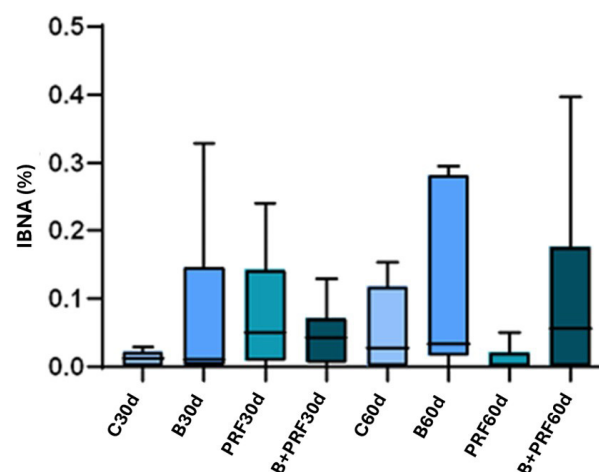


Figure 7 - Maximum and minimum value, median, 1st and 3rd quartile of the Intramembranous Neoformation Area (IBNA) in percentage.

significant difference from group PRF (C vs. PRF, $p=0.0374$); which, in turn, presented itself as similar to groups B+PRF and B, although group B+PRF has the second lowest value within the variable. At 60 days, group C showed a statistical difference compared to group B (C vs. B, $p=0.0374$), the other groups did not show a statistical difference, and only group B showed a statistically significant difference within the intragroup analysis (B30 vs. B60, $p=0.0313$) (Figure 8).

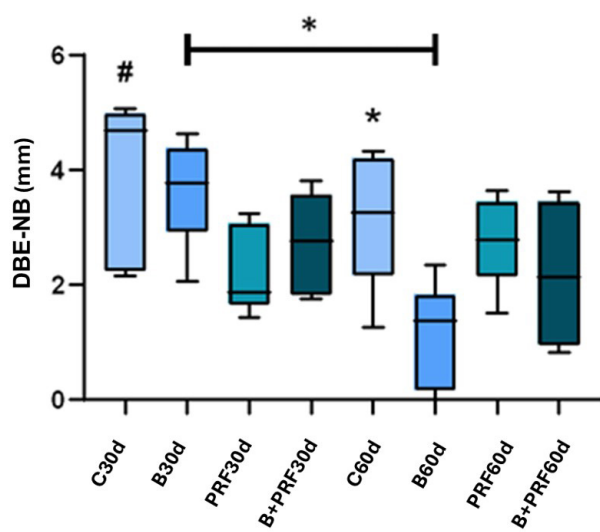


Figure 8 - Maximum and minimum value, median, 1st and 3rd quartile of the distance between neoformed bone edges (DBE-NB) in mm. Statistically significant intragroup and intergroup difference for Group B (*), intergroup for Group PRF (#).

Immunohistochemical analysis

In the RANKL analysis, 30 days after surgery, the presence of immunostaining cells was observed in all specimens, especially in the B+PRF group. In some specimens of the B+PRF group, it was also possible to visualize immunostaining cells located between the spaces of the remaining biomaterial particles (Figure 9). At 60 days, all specimens presented cells with biomarker immunostaining. A reduced number of immunostaining cells was noted in the C and PRF groups, while in the B group the number of cells was higher (Figure 9).

In the OPG analysis, 30 days after surgery, the presence of immunostaining cells was observed in most specimens, especially in the B and B+PRF groups. In some specimens of these groups, cells were observed distributed between the spaces of the remaining biomaterial particles. However, the PRF group exhibited a less standardized cell distribution (Figure 10). At 60 days, most specimens revealed biomarker immunostaining cells. A smaller number of cells was noted in the C and PRF groups, while the B group presented a higher quantity of immunostaining cells (Figure 10).

In the TRAP analysis, 30 days after surgery, the presence of immunostaining cells was observed in all specimens, especially in the C and B groups. In some specimens of the B group, it was

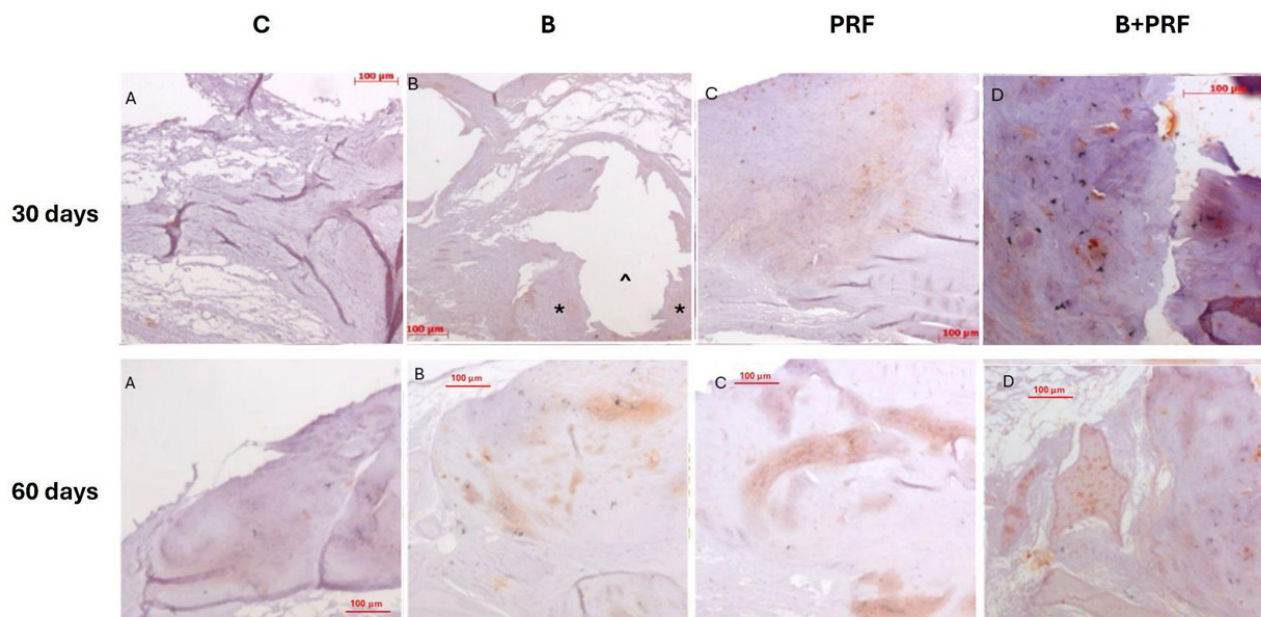


Figure 9 - Photomicrographs of histological sections with positive immunostaining for RANKL (hematoxylin and eosin staining, original magnification X10) - (30 days) (A) group C, (B) group B- * immunostaining area surrounding spaces of the remaining biomaterial particles ^, (C) group PRF, (D) group B+PRF; (60 days) (A) group C, (B) group B, (C) group PRF, (D) group B+PRF.

possible to visualize immunostaining cells located between the spaces of the remaining biomaterial particles, and the other groups presented a more irregular presence of immunostaining cells (Figure 11). At 60 days, all specimens presented biomarker immunostaining cells. A reduced number of immunostaining cells was noted in the PRF and B+PRF groups, while in the B and C

groups the number of immunostaining cells was higher (Figure 11).

The RANKL analysis of moderate immunostaining cells revealed that, when the factors time, 30 and 60 days, were evaluated, there was no difference between the immunostaining pattern considering the periods. The highest intensity of

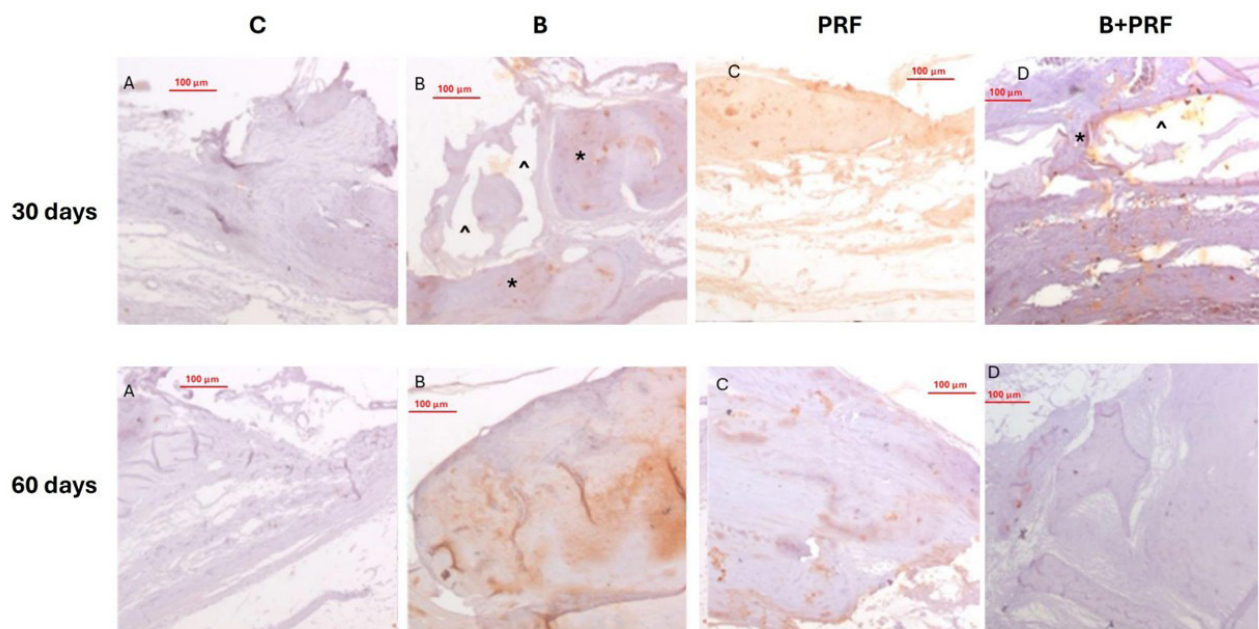


Figure 10 - Photomicrographs of histological sections with immunostaining positive for OPG (hematoxylin and eosin staining, original magnification X10) - (30 days) (A) group C, (B) group B, (C) group PRF, (D) group B+PRF. * immunostaining area surrounding spaces of the remaining biomaterial particles ^; (60 days) (A) group C, (B) group B, (C) group PRF, (D) group B+PRF.

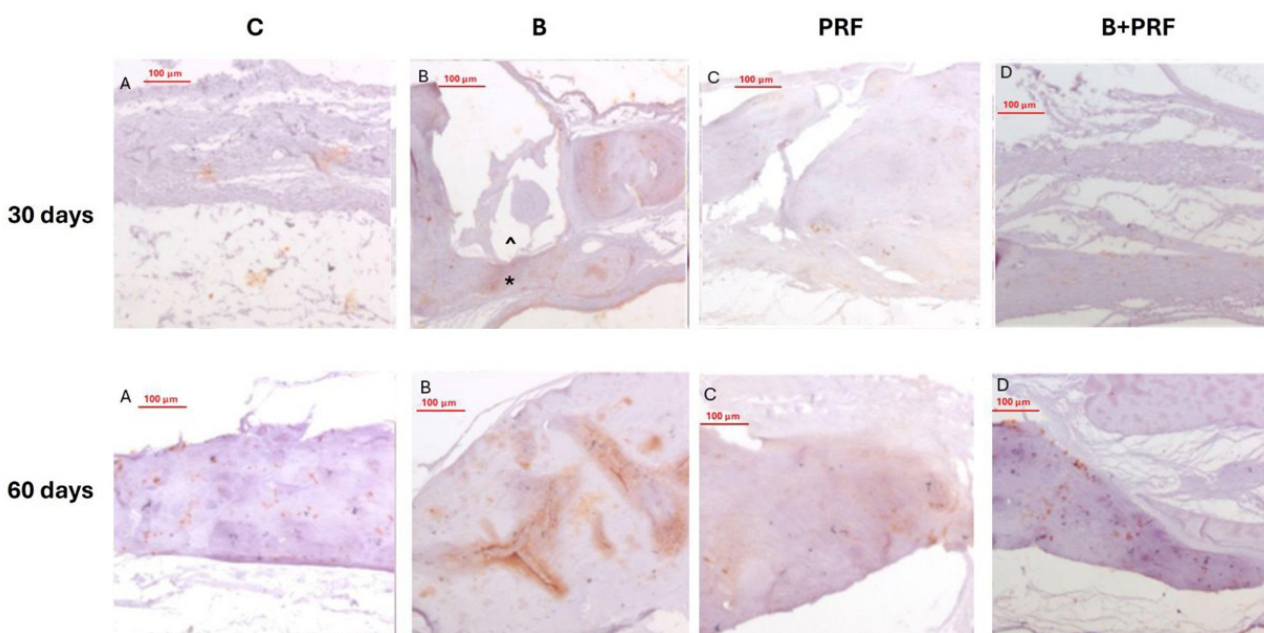


Figure 11 - Photomicrographs of histological sections with positive immunostaining for TRAP (hematoxylin and eosin staining, original magnification X10) - (30 days) (A) group C, (B) group B * immunostaining area surrounding spaces of the remaining biomaterial particles ^, (C) group PRF, (D) group B+PRF; (60 days) (A) group C, (B) group B, (C) group PRF, (D) group B+PRF.

immunostaining was observed in groups B and B+PRF at 60 days (B 60 x B30 $p<0.0001$, B+PRF 60 x B+PRF 30 $p=0.008$) (Figure 12).

The OPG analysis of moderate immunostaining cells revealed that, when the factors time, 30 and 60 days were evaluated, the highest intensity of immunostaining was observed in groups B 60 (B60 x B30 $p\leq0.0001$), PRF 60 (PRF60 x

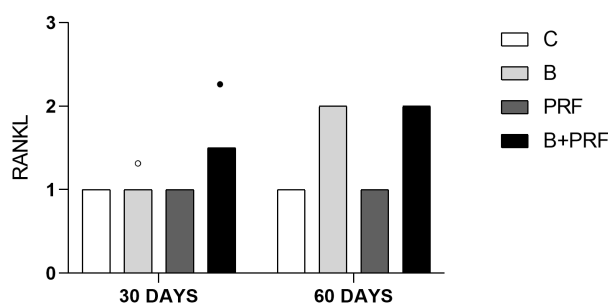


Figure 12 - Graph of medias range of the area of moderate immunostaining expression for RANKL (◦) statistical difference showing higher expression of RANKL in B60 compared to B30, (▪) statistical difference showing greater RANKL immunolabeling in B+PRF60 compared to B+PRF30. Two-way ANOVA, $p<0.05$.

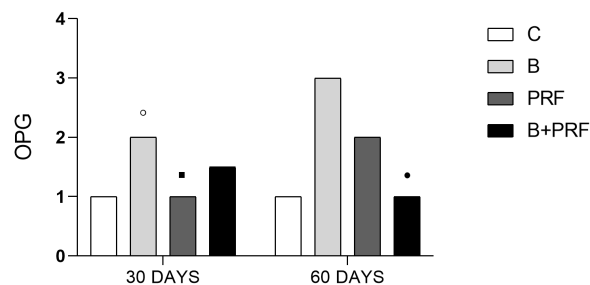


Figure 13 - Graph of medias range of the area of moderate immunostaining expression for OPG (◦) statistical difference showing higher OPG expression in B 60 compared to B 30, (▪) statistical difference showing higher OPG expression in PRF 60 compared to PRF 30, and (•) statistical difference showing higher OPG expression in B+PRF 30 compared to B+PRF 60) Two-way ANOVA, $p<0.05$.

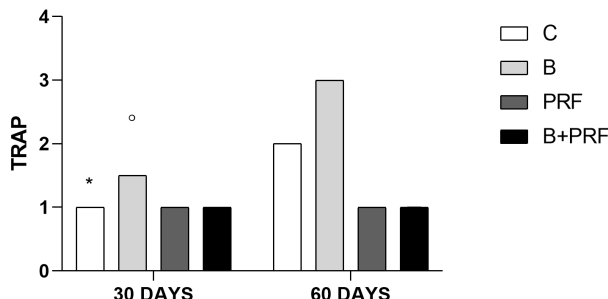


Figure 14 - Graph of medias range of the area of moderate immunostaining expression for TRAP (*) statistical difference showing higher TRAP expression in C 60 compared to C 30, (◦) statistical difference showing higher TRAP expression in B 60 compared to B 30). Two-way ANOVA, $p<0.05$.

PRF30, $p\leq0.0001$) and B+PRF 30 (B+PRF 30 x B+PRF 60, $p=0.0081$) (Figure 13).

The TRAP analysis of moderate immunostaining cells revealed that, at 30 days, when the factors time, 30 and 60 days, were evaluated, the highest intensity of immunostaining was observed in groups C 60 (C 60 x C30 $p<0.0001$) and B 60 (B 60 x B 30 $p<0.0001$) (Figure 14).

DISCUSSION

The aim of this study was to evaluate, through histomorphometric and immunohistochemical analysis, the bone repair of critical size defects in rats treated with bovine bone mineral matrix (Bio-Oss®) and platelet-rich fibrin.

In previous studies, the association of Bio-Oss® with PRF showed superior results compared to the individual treatment groups within a period of 30 days when compared to the proportion of bone neoformation [9,26]. However, the better histological performance by PRF only at 30 days presented in this study can be explained by the greater amount of growth factors that PRF releases in the first 28 days [27], and that in defects filled with Bio-Oss®, a greater amount of bone formation was observed with longer periods of follow-up [9]. In addition, there is no evidence showing that the PRF membrane can maintain the space for tissue regeneration for sufficient periods, due to its rapid degradation [28].

Oliveira et al. (2015) [9] and do Lago et al. (2020) [26] concluded that Bio-Oss® associated with PRF has a higher proportion of bone neoformation compared to the use of an isolated membrane, which diverges from the results of the present study since there was not a statistical difference when comparing groups PRF and B+PRF. This divergence of results can be an effect due to the difference in the ways of using fibrin, while Oliveira et al. (2015) [9] and Lago et al. (2020) [26] used PRF as a filling material mixed with the biomaterial, the present study used fibrin as a membrane, just covering the region of the surgical defect.

Histologically, a certain disparity was observed regarding the presence of particles or their remaining spaces within the surgical defect between specimens in group B and group B+PRF. While particles in group B were scarce, in group B+PRF the presence of the biomaterial inside the defect was recurrent, suggesting that the PRF

membrane act as a maintainer of the particles inside the defect. Ondur et al. (2020) [29] concluded that the use of PRF mixed with the biomaterial and as a membrane provides a similar bone regeneration pattern compared to the use of the biomaterial in combination with a collagen membrane. In addition, the use of PRF may be preferred due to its autogenous origin, being cheaper than collagen membrane, and being easy to use.

At 30 days, on the proportional variable of the area of lamellar bone neoformation (LBNA%), group PRF performed better than group B, while the remaining groups were statistically similar. At 60 days, there was no statistically significant difference between the treatment modalities. The release of growth factors by fibrin occurs slowly and gradually [30,31], taking place between the first week and 28 days after its application [27]. This release of growth factors in the early period has a great influence on the bone repair process; since the growth factors present in PRF, such as platelet-derived growth factor, transforming growth factor, insulin-like growth factor, the factor of fibroblast growth, and epithelial growth factor, during the healing process are known to promote angiogenesis, in addition to contributing to matrix synthesis, cell differentiation, and new bone formation through osteoblasts [11,22,32,33].

The treatment groups presented similar statistical results regarding the proportion of intramembranous neoformation area (IBNA%). However, it is possible to observe that at 30 days, groups B and PRF had better values, as compared to 60 days, group B+PRF has an improvement within the variable as group B maintains great results. These data may be associated with the ability of Bio-Oss® to act as a scaffold, maintaining a viable space for vascular infiltration and the internal migration of cellular elements involved in bone formation, such as undifferentiated mesenchymal cells, osteoblasts, and osteoclasts [26], having a positive influence on bone neoformation located in the central region of the surgical defect.

By scanning microscopy, Bio-Oss® shows macro topography with interconnected macropores with dotted nanostructures, made of granules with a size of almost 50–100 nm in diameter. The presence of these micro and nanostructures is important due to the increase in surface area, which helps in the adsorption of growth factors and proteins that can trigger new bone formation [34], which would justify the data

presented here. Bio-Oss® actively participates in bone neoformation and remodeling processes through its osteoconductive action, which supports the maintenance of the original bone architecture.

The presence of blood supply from bone native spinal cord has a major influence on the pattern of bone neoformation [35]. In the present study, the bone neoformation area was concentrated close to the edges of the surgical defects and extended to the central region; this pattern can be observed on the parameters of LBNA and IBNA. As Oliveira et al. (2015) [9], none of the groups presented in the present study performed the complete wound closure until 60 days.

The linear variable of the distance between neoformed bone edges (DBE-NE mm) determines the remaining distance between the edges of the newly formed bone, which allows to assess the closure of surgical defects. In the present study, it is possible to observe that the control group had the worst performance in this parameter. Overall, the treatments applied showed potential action to close the defect, with group PRF being highlighted at 30 days and group B at 60 days. Despite this, no treatment modality achieved complete closure of the defect at the end of the study. The ability of Bio-Oss® to act on defect closure has been previously reported [24].

For the RANKL biomarker at 60 days, it can be seen that groups B and B+PRF are the ones with the highest intensity of marking, a fact that can be attributed to the very presence of the biomaterial (Bio-Oss®). The expression of RANKL was considered moderate and may be portraying a stimulus to cell differentiation in osteoclasts and not necessarily connoting osteoclastic activity. These findings corroborate the study by Torquato et al. (2021) [24], in which there was moderate expression of RANKL in the groups associated with Bio-Oss®.

Groups B and PRF showed the highest expression of the OPG biomarker at 60 days, while group B+PRF showed the highest expression of OPG at 30 days. This suggests that the release of growth factors in the early stages of repair may have enhanced the effect of the xenogeneic graft (Bio-Oss®). Despite the statistical differences in the intensity of expression of the OPG biomarker between the study groups, there is evidence of OPG expression throughout the analysis period, i.e. during the 60 days, indicating a process of bone

neoformation consistent with the data from the histomorphometric analysis.

In terms of osteoclastic activity, the PRF and B+PRF groups showed the lowest expression of TRAP, suggesting that the presence of the PRF membrane may lead to lower osteoclastic activity.

The data presented in this study should be carefully analyzed, as it has some limitations. One of the limitations would be the absence of an initial observation period, close to 15 days after surgery, as this analysis could provide important data on the beginning of repair in all study groups, especially fibrin. For this study, the observation periods chosen made it possible to analyze the bone repair capacity in bone defects in the long term, and it was found, despite its limitations, that, as in the study by Oliveira et al. (2015) [9], Bio-Oss® showed significant bone neoformation after 60 days. In addition, the preparation of platelet-rich fibrin can have a great influence on the results and makes the comparison between studies challenging, since there is considerable variation in the literature in the way fibrin is obtained, as well as in the observation periods and models of animals used.

This study introduces an innovative approach to bone regeneration by combining mineralized bovine bone matrix (Bio-Oss®) with platelet-rich fibrin (PRF) applied specifically as a biological membrane. Unlike previous protocols where PRF was mixed with graft materials [12], this study allows a distinct evaluation of PRF's barrier effect in maintaining graft stability and promoting a favorable environment for bone healing. In addition to its containment role, PRF acts as an autologous source of growth factors, enhancing cell recruitment, angiogenesis, and osteogenic differentiation, while offering a safe, low-cost, and biocompatible alternative.

The inclusion of detailed histomorphometric and immunohistochemical analyses (RANKL, OPG, TRAP) provides new insights into the cellular mechanisms regulating bone repair, linking bone formation dynamics with osteoblastic and osteoclastic activity. Thus, this study contributes to the development of more effective regenerative protocols with direct translational potential for clinical applications in implantology and bone defect treatment.

Therefore, further studies should be carried out to investigate the bone repair capacity of biomaterials, with different analysis periods and

with analysis of bone formation biomarkers, in addition to those used in the present study (OPG, TRAP and RANKL) other biomarkers important for understanding bone biology can be explored, such as osteopontin (OPN), osteocalcin (OC), osteonectin (SPARC), bone sialoprotein (BSP), Runt-related transcription factor 2 (Runx2), among others, thus being able to transpose the results into future clinical practice.

CONCLUSION

Considering the proposed methodology, the evaluation periods, and the results obtained in this study, it was possible to conclude that platelet-rich fibrin has a positive action on the initial process of bone repair and neoformation. Meanwhile, the association of Bio-Oss® xenograft with platelet-rich fibrin seems to be more related to the maintenance of the new bone formation architecture. However, more studies are needed to confirm this finding.

Author's Contributions

EACS, LCT, ACDM: Investigation. EACS, LCT, ACDM: Data Curation. EACS, LCT, LOM, CMMN, ACDM: Methodology. EACS, LCT: Writing – Original Draft Preparation. EACS, LCT, LOM, CMMN, ACDM: Formal Analysis. KAP, CCMM, NDA, ACDM: Writing – Review & Editing. MANJ, MPS, ACDM: Supervision. ACDM: Conceptualization. ACDM: Project Administration.

Conflict of Interest

No conflicts of interest declared concerning the publication of this article.

Funding

The authors declare that no financial support was received.

Regulatory Statement

Not applicable.

REFERENCES

1. Springfield DS. Autogenous bone grafts: nonvascular and vascular. *Orthopedics*. 1992;15(10):1237-41. <http://doi.org/10.3928/0147-7447-19921001-14>. PMID:1409132.
2. Khouri RK, Brown DM, Koudsi B, Deune EG, Gilula LA, Cooley BC, et al. Repair of calvarial defects with flap tissue: role of bone morphogenetic proteins and competent responding

tissues. *Plast Reconstr Surg.* 1996;98(1):103-9. <http://doi.org/10.1097/00006534-199607000-00017>. PMid:8657761.

3. Chaushu G, Mardinger O, Calderon S, Moses O, Nissan J. The use of cancellous block allograft for sinus floor augmentation with simultaneous implant placement in the posterior atrophic maxilla. *J Periodontol.* 2009;80(3):422-8. <http://doi.org/10.1902/jop.2009.080451>. PMid:19254126.
4. Sbordone L, Toti P, Menchini-Fabris G, Sbordone C, Guidetti F. Implant success in sinus-lifted maxillae and native bone: a 3-year clinical and computerized tomographic follow-up. *Int J Oral Maxillofac Implants.* 2009;24(2):316-24. PMid:19492648.
5. Schmitt CM, Doering H, Schmidt T, Lutz R, Neukam FW, Schlegel KA. Histological results after maxillary sinus augmentation with Straumann® BoneCeramic, Bio-Oss®, Puros®, and autologous bone. A randomized controlled clinical trial. *Clin Oral Implants Res.* 2013;24(5):576-85. <http://doi.org/10.1111/j.1600-0501.2012.02431.x>. PMid:22324456.
6. Iezzi G, Scarano A, Mangano C, Cirotti B, Piattelli A. Histologic results from a human implant retrieved due to fracture 5 years after insertion in a sinus augmented with anorganic bovine bone. *J Periodontol.* 2008;79(1):192-8. <http://doi.org/10.1902/jop.2008.070105>. PMid:18166111.
7. Stavropoulos A, Kostopoulos L, Nyengaard JR, Karring T. Deproteinized bovine bone (Bio-Oss) and bioactive glass (Biogran) arrest bone formation when used as an adjunct to guided tissue regeneration (GTR): an experimental study in the rat. *J Clin Periodontol.* 2003;30(7):636-43. <http://doi.org/10.1034/j.1600-051X.2003.00093.x>. PMid:12834502.
8. Li Y, Yang L, Zheng Z, Li Z, Deng T, Ren W, et al. Bio-Oss® modified by calcitonin gene-related peptide promotes osteogenesis in vitro. *Exp Ther Med.* 2017;14(5):4001-8. <http://doi.org/10.3892/etm.2017.5048>. PMid:29067095.
9. Oliveira MR, Silva AC, Ferreira S, Avelino CC, Garcia IR Jr, Mariano RC. Influence of the association between platelet-rich fibrin and bovine bone on bone regeneration. A histomorphometric study in the calvaria of rats. *Int J Oral Maxillofac Surg.* 2015;44(5):649-55. <http://doi.org/10.1016/j.ijom.2014.12.005>. PMid:25553712.
10. Borie E, Oliví DG, Orsi IA, Garlet K, Weber B, Beltrán V, et al. Platelet-rich fibrin application in dentistry: a literature review. *Int J Clin Exp Med.* 2015;8(5):7922-9. PMid:26221349.
11. Dohan DM, Choukroun J, Diss A, Dohan SL, Dohan AJJ, Mouhyi J, et al. Platelet-rich fibrin (PRF): a second-generation platelet concentrate. Part II: platelet-related biologic features. *Oral Surg Oral Med Oral Pathol Oral Radiol Endod.* 2006;101(3):e45-50. <http://doi.org/10.1016/j.tripleo.2005.07.009>. PMid:16504850.
12. Nacopoulos C, Dontas I, Lelovas P, Galanos A, Vesalas A-M, Raptou P, et al. Enhancement of bone regeneration with the combination of platelet-rich fibrin and synthetic graft. *J Craniofac Surg.* 2014;25(6):2164-8. <http://doi.org/10.1097/SCS.0000000000001172>. PMid:25318438.
13. Pripatnanont P, Nuntanaranont T, Vongvcharanont S, Phurisat K. The primacy of platelet-rich fibrin on bone regeneration of various grafts in rabbit's calvarial defects. *J Craniomaxillofac Surg.* 2013;41(8):191-200. <http://doi.org/10.1016/j.jcms.2013.01.018>. PMid:23395296.
14. Carneiro BGDS, Maia TAC, Costa V, Friedrichsdorf SP, Gondim DV, Pereira KMA, et al. Platelet-rich fibrin associated to bovine bone induces bone regeneration in model of critical-sized calvaria defect of rats submitted to Zoledronic Acid therapy: PRF induces bone healing. *J Stomatol Oral Maxillofac Surg.* 2024; 126(4S):102175. <http://doi.org/10.1016/j.jormas.2024.102175>. PMid:39631530.
15. You JS, Kim SG, Oh JS, Kim JS. Effects of platelet-derived material (Platelet-Rich Fibrin) on bone regeneration. *Implant Dent.* 2019;28(3):244-55. <http://doi.org/10.1097/ID.0000000000000877>. PMid:31124821.
16. Shalaby LS, Shawkat S, Fathy I. Potential effect of platelet rich fibrin prepared under different centrifugation protocols on stem cells from the apical papilla. *Braz Dent Sci.* 2023;26(4):e3847. <http://doi.org/10.4322/bds.2023.e3847>.
17. Augustina EF, Rivai NR, Gifary HM. The expression of matrix metalloproteinase-13 (MMP-13) on xenograft and PRF in bone regeneration. *Braz Dent Sci.* 2023;26(2):e3366. <http://doi.org/10.4322/bds.2023.e3366>.
18. Dohan Ehrenfest DM, Rasmussen L, Albrektsson T. Classification of platelet concentrates: from pure platelet-rich plasma (P-PRP) to leucocyte- and platelet-rich fibrin (L-PRF). *Trends Biotechnol.* 2009;27(3):158-67. <http://doi.org/10.1016/j.tibtech.2008.11.009>. PMid:19187989.
19. Percie du Sert N, Hurst V, Ahluwalia A, Alam S, Avey MT, Baker M, et al. The ARRIVE guidelines 2.0: updated guidelines for reporting animal research. *PLoS Biol.* 2020;18(7):e3000410. <http://doi.org/10.1371/journal.pbio.3000410>. PMid:32663219.
20. Calixto JC, Lima CEVC, Frederico L, Lima RP, Anbinder AL, Lima RPSC, et al. The influence of local administration of simvastatin in calvarial bone healing in rats. *J Craniomaxillofac Surg.* 2011;39(3):215-20. <http://doi.org/10.1016/j.jcms.2010.03.009>. PMid:20456964.
21. Nagata MJH, Santinoni CS, Pola NM, de Campos N, Messora MR, Bomfim SRM, et al. Bone marrow aspirate combined with low-level laser therapy: A new therapeutic approach to enhance bone healing. *J Photochem Photobiol B.* 2013;121:6-14. <http://doi.org/10.1016/j.jphotobiol.2013.01.013>. PMid:23474527.
22. Dohan Ehrenfest DM, Diss A, Odin G, Doglioli P, Hippolyte MP, Charrier JB. In vitro effects of Choukroun's PRF (platelet-rich fibrin) on human gingival fibroblasts, dermal prekeratinocytes, preadipocytes, and maxillofacial osteoblasts in primary cultures. *Oral Surg Oral Med Oral Pathol Oral Radiol Endod.* 2009;108(3):341-52. <http://doi.org/10.1016/j.tripleo.2009.04.020>. PMid:19589702.
23. Messora MR, Nagata MJ, Dornelles RC, Bomfim SR, Furlaneto FA, de Melo LG, et al. Bone healing in critical-size defects treated with platelet-rich plasma activated by two different methods. A histologic and histometric study in rat calvaria. *J Periodontal Res.* 2008;43(6):723-9. <http://doi.org/10.1111/j.1600-0765.2008.01084.x>. PMid:18705653.
24. Torquato LC, Suárez EAC, Bernardo DV, Pinto ILR, Mantovani LO, Silva TIL, et al. Bone repair assessment of critical size defects in rats treated with mineralized bovine bone (Bio-Oss®) and photobiomodulation therapy: a histomorphometric and immunohistochemical study. *Lasers Med Sci.* 2021;36(7):1515-25. <http://doi.org/10.1007/s10103-020-03234-5>. PMid:33400010.
25. Buduneli E, Vardar-Sengül S, Buduneli N, Atilla G, Wahlgren J, Sorsa T. Matrix metalloproteinases, tissue inhibitor of matrix metalloproteinase-1, and laminin-5 g2 chain immunolocalization in gingival tissue of endotoxin-induced periodontitis in rats: effects of low-dose doxycycline and alendronate. *J Periodontol.* 2007;78(1):127-34. <http://doi.org/10.1902/jop.2007.050451>.
26. Lago ES, Ferreira S, Garcia IR Jr, Okamoto R, Mariano RC. Improvement of bone repair with I-PRF and bovine bone in calvaria of rats. Histometric and immunohistochemical study. *Clin Oral Investig.* 2020;24(5):1637-50. <http://doi.org/10.1007/s00784-019-03018-4>. PMid:31338633.
27. Kang YH, Jeon SH, Park JY, Chung JH, Choung YH, Choung HW, et al. Platelet-rich fibrin is a Biscay fold and reservoir of growth factors for tissue regeneration. *Tissue Eng Part A.* 2011;17(3-4):349-59. <http://doi.org/10.1089/ten.tea.2010.0327>. PMid:20799008.
28. Kawase T, Kamiya M, Kobayashi M, Tanaka T, Okuda K, Wolff LF, et al. The heat-compression technique for the conversion of platelet-rich fibrin preparation to a barrier membrane with a reduced rate of biodegradation. *J Biomed Mater Res B Appl Biomater.* 2015;103(4):825-31. <http://doi.org/10.1002/jbm.b.33262>. PMid:25132655.
29. Ondur E, Balcioglu NB, Tekkesin MS, Guzel O, Ersanli S. Effects of platelet-rich fibrin on hard tissue healing: a histomorphometric

crossover trial in sheep. Materials. 2020;13(7):1695. <http://doi.org/10.3390/ma13071695>. PMid:32260464.

30. Wu CL, Lee SS, Tsai CH, Lu KH, Zhao JH, Chang YC. Platelet-rich fibrin increase cell attachment, proliferation and collagen – related protein expression of human osteoblasts. *Aust Dent J.* 2012;57(2):207-12. <http://doi.org/10.1111/j.1834-7819.2012.01686.x>. PMid:22624763.

31. Zhang Y, Tangl S, Huber CD, Lin Y, Qiu L, Rausch-Fan X. Effects of Choukroun's platelet-rich fibrin on bone regeneration in combination with desproteinized bovine bone mineral in maxillary sinus augmentation. A histological and histomorphometric study. *J Craniomaxillofac Surg.* 2012;40(4):321-8. <http://doi.org/10.1016/j.jcms.2011.04.020>. PMid:21664828.

32. Choukroun J, Diss A, Simonpieri A, Girard MO, Schoeffler C, Dohan SL, et al. Platelet-rich fibrin (PRF): a secondgeneration platelet concentrate. Part IV: Clinical effects on tissue healing. *Oral Surg*

Oral Med Oral Pathol Oral Radiol Endod. 2006;101(3):e56-60. <http://doi.org/10.1016/j.tripleo.2005.07.011>. PMid:16504852.

33. Nagareddy PR, Lakshmana M. Withania somnifera improves bone calcification in calcium-deficient ovariectomized rats. *J Pharm Pharmacol.* 2006;58(4):513-9. <http://doi.org/10.1211/jpp.58.4.0011>. PMid:16597369.

34. Fan YP, Lu JF, Xu AT, He FM. Physicochemical characterization and biological effect of anorganic bovine bone matrix and organic-containing bovine bone matrix in comparison with Bio-Oss in rabbits. *J Biomater Appl.* 2018;33(4):566-75. <http://doi.org/10.1177/0885328218804926>. PMid:30326803.

35. Rasouli Ghahroudi AA, Rokn AR, Kalhori KAM, Khorsand A, Pournabi A, Pinheiro ALB, et al. Effect of low-level laser therapy irradiation and Bio-Oss graft material on the osteogenesis process in rabbit calvarium defects: a double blind experimental study. *Lasers Med Sci.* 2014;29(3):925-32. <http://doi.org/10.1007/s10103-013-1403-5>. PMid:23996072.

Andrea Carvalho De Marco
(Corresponding address)

Universidade Estadual Paulista, Departamento de Diagnóstico e Cirurgia, São José dos Campos, SP, Brazil.
Email: andrea.marco@unesp.br

Editor: Renata Falchete do Prado

Date submitted: 2025 May 08
Accept submission: 2025 Jul 29